Eur. Phys. J. B **27**, 577–582 (2002)
DOI: 10.1140/epjb/e2002-00192-y

THE EUROPEAN PHYSICAL JOURNAL B

Surface and interface optical phonon modes and electron-phonon interaction in a multi-shell spherical system

Li Zhang[1,a], Hong-Jing Xie[1,2], and Chuan-Yu Chen[1]

[1] Department of Physics, Guihuagang Campus, Guangzhou University, Guangzhou 510405, PR China
[2] Department of Physics, Beijing Normal University, Beijing 100875, PR China

Received 16 October 2001 and Received in final form 23 January 2002
Published online 25 June 2002

Abstract. Within the framework of the dielectric continuum model, interface optical(IO) and surface optical(SO) phonon modes and the Fröhlich electron-IO (SO) phonon interaction Hamiltonian in a multi-shell spherical system were derived and studied. Numerical calculation on CdS/HgS/H_2O and CdS/HgS/CdS/H_2O spherical systems have been performed. Results reveal that there are two IO modes and one SO mode for the CdS/HgS/H_2O system, one SO mode and four IO modes whose frequencies approach the IO phonon frequencies of the single CdS/HgS heterostructure with the increasing of the quantum number l for CdS/HgS/CdS/H_2O. It also showed that smaller l and SO phonon compared with IO phonon, have more significant contribution to the electron-IO (SO) phonon interaction.

PACS. 74.25.Kc Phonons – 71.38.-k Polarons and electron-phonon interactions – 63.20.Kr Phonon-electron and phonon-phonon interactions

1 Introduction

In recent years, due to the great progress in semiconductor nanotechnology, such as molecular-beam epitaxy, metal-organic chemical-vapor deposition, many sophisticated semiconductor heterostructures, for example, the multi-layer planar quantum wells (QW), multi-layer cylindrical quantum well wire (QWW), and multi-layer spherical quantum dot quantum well (QDQW) [1–3] can be fabricated. It is well known that the phonon contribution plays an important role in effecting the physical properties such as the electronic energy level, the bound energies of impurity and the carrier transportation in these reduced-dimensional systems. Several authors have made their contributions in studying the phonon modes and electron-phonon interaction in various low dimensional quantum systems. Mori and Ando [4] have investigated the phonon modes in single and double heterostructure QWs within the framework of a dielectric continuum (DC). Jun-jie Shi *et al.* [5,6] have studied the phonon modes in the coupled and step QWs with four and five layers of GaAs/$Al_xGa_{1-x}As$, the electron-phonon interaction Fröhlich Hamiltonian were also given and the electron-interface phonon coupling functions were discussed. Constantinou and Ridley [7] have investigated the guided and interface optical phonon in cylindrical QWW by using a dispersive hydrodynamic continuum theory, and the dispersion relations and phonon potential functions distribution were discussed. Recently, Xie *et al.* [8,9] have studied the phonon modes in QWWs with infinite and finite potential boundary conditions and derived the electron-phonon interaction Hamiltonians. Klimin *et al.* [10] have determined the vibrational modes of inertial polarization in the multilayer QWW and quantum dot (QD). Klein *et al.* [11] have deduced phonon modes and electron-phonon interaction Hamiltonian in spherical QD. Roca and coworkers [12] have investigated the optical vibrational modes in a QD by a macroscopic continuum, coupling the mechanical vibrational amplitude and electrostatic potential. Tkach *et al.* [13] have studied the spherical nanoheterosystem: CdS/HgS/H_2O, the phonon modes were obtained under the DC model.

In the works mentioned above, the analytical macroscopic modes such as the hydrodynamic model [7] and DC model [4,10,11,13] had been employed, and the models had their limits in describing optical modes in quantum well structures. But as pointed out by Kun Huang *et al.* [14], under the long-wavelength limit of the optical vibrations and ignoring the dispersion of the bulk longitudinal-optical (LO) and transverse-optical (TO) phonons, the microscopic model and the DC model agreed completely. Moreover, Rücker *et al.* [15,16] calculated the electron-optical phonon scattering rates on the basis of microscopic descriptions of the phonon spectra, results reveals that the slab [4] and HZ [14] modes agree fairly

[a] e-mail: zhangli-gz@263.net

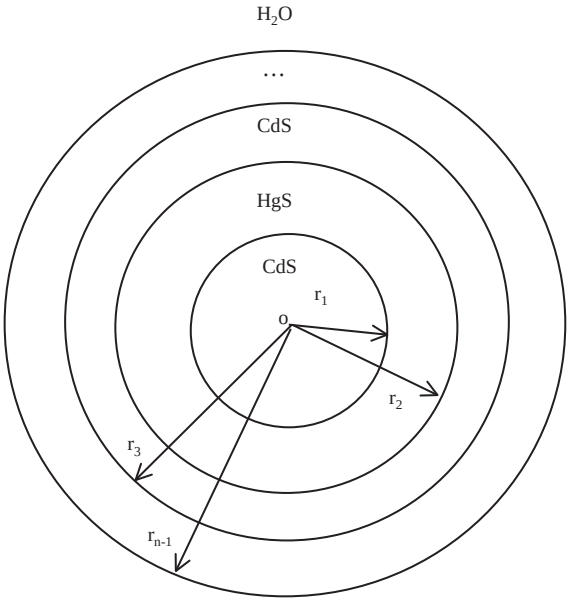

Fig. 1. The schematic structure of the multilayer spherical system.

well with the microscopic calculation. Because of the simplicity and efficiency of the DC modes, especially for the polaron effects [8,9], we will use it to study the optical phonon modes in a multi-shell spherical system.

In general, there were some confined LO phonon modes and some interface optical (IO) or surface optical (SO) phonon modes in multi-layer heterostructure quantum systems, but the couplings between the IO (or SO) phonons and electrons were stronger compared with the couplings between the LO phonons and electrons [6,8,9]. For the sake of simplicity, in the present paper, we will only investigate the properties of the IO or SO phonon modes in an n-layer spherical nanoheterosystem. The advantage of this work is that, for an n-layer shell spherical system, (1) we have derived the orthonormal relation for the polarization vector, (2) through the orthonormal relation and the dynamic equation of motion of the crystal lattice, the Fröhlich electron-phonon interaction Hamiltonian has been derived, (3) from the discussions of the IO (SO) phonon dispersion relations, phonon potential distributions, and the electron-phonon coupling functions for 3-layer and 4-layer systems, the characters of IO (SO) phonon modes for an n-layer shell spherical system have been concluded. The schema of our model is given in Figure 1.

The paper is organized as follows: the IO and SO phonon dispersion relations and the Fröhlich electron-IO (SO) phonon interaction Hamiltonian were deduced in Section 2; As an example, the numerical results for the dispersion relation, the electron-phonon coupling functions for three layers of CdS/HgS/H_2O and four layers of CdS/HgS/CdS/H_2O spherical system were given and discussed in Section 3; In Section 4, we summarized the main results and gave some extended conclusions.

2 Theory

Under the DC approximation, taking the phonon potential couplings between the IO and SO phonons into account, the IO and SO phonon potential in an n-layer shell spherical system can be written as

$$\phi(\mathbf{r}) = \begin{cases} A_1 r^l Y_{lm}(\theta,\varphi) & 0 < r \le r_1 \\ (A_2 r^l + B_2 r^{-l-1}) Y_{lm}(\theta,\varphi) & r_1 < r \le r_2 \\ \cdots & \cdots \\ (A_i r^l + B_i r^{-l-1}) Y_{lm}(\theta,\varphi) & r_{i-1} < r \le r_i \\ \cdots & \cdots \\ B_n r^{-l-1} Y_{lm}(\theta,\varphi) & r_{n-1} < r < \infty \end{cases}. \tag{1}$$

The phonon potential function and the normal component of electric displace continuum at $r = r_i (i = 1, 2 \text{ to } n-1)$ imply

$$\begin{cases} \phi_{ilm}|_{r=r_i} = \phi_{i+1,lm}|_{r=r_i} \\ \varepsilon_i(\omega) \frac{\partial \phi_{ilm}}{\partial r}|_{r=r_i} = \varepsilon_{i+1}(\omega) \frac{\partial \phi_{i+1,lm}}{\partial r}|_{r=r_i} \end{cases}, i = 1, 2 \text{ to } n-1 \tag{2}$$

with the dielectric function $\varepsilon_i(\omega)$ given by

$$\varepsilon_i(\omega) = \varepsilon_{i\infty} + \frac{\varepsilon_{i0} - \varepsilon_{i\infty}}{1 - \omega^2/\omega_{TOi}^2}, \; i = 1, 2 \text{ to } n-1, \tag{3}$$

$$\varepsilon_n = \varepsilon_d \tag{4}$$

where ε_{i0}, $\varepsilon_{i\infty}$ are the static and high-frequency dielectric constants of ith layer material, ω_{TOi} is the corresponding frequency of transverse-optical vibration, and ε_d is the dielectric constant of the outer layer nonpolar surrounding. We define

$$\begin{aligned} &\varepsilon_i l r_i^{l-1} = f_i, \\ &\varepsilon_{i+1} l r_i^{l-1} = f_i', \\ &\varepsilon_i (l+1) r_i^{-l-2} = g_i, \\ &\varepsilon_{i+1} (l+1) r_i^{-l-2} = g_i', \\ &r_i^l = h_i, \\ &r_i^{-l-1} = h_i', \end{aligned} \tag{5}$$

then the dispersion relation of IO and SO phonon was obtained *via* the below $(2n-2)\times(2n-2)$ determinant (6)

$$\begin{vmatrix} h_1 & -h_1 & -h_1' & 0 & 0 & 0 & 0 & 0 & 0 & 0 & 0 \\ f_1 & -f_1' & g_1' & 0 & 0 & 0 & 0 & 0 & 0 & 0 & 0 \\ 0 & h_2 & h_2' & -h_2 & -h_2' & 0 & 0 & 0 & 0 & 0 & 0 \\ 0 & f_2 & -g_2 & -f_2' & g_2' & 0 & 0 & 0 & 0 & 0 & 0 \\ 0 & 0 & 0 & 0 & 0 & \ldots & 0 & 0 & 0 & 0 & 0 \\ 0 & 0 & 0 & 0 & 0 & 0 & h_{n-2} & h_{n-2}' & -h_{n-2} & -h_{n-2}' & 0 \\ 0 & 0 & 0 & 0 & 0 & 0 & f_{n-2} & -g_{n-2} & -f_{n-2}' & g_{n-2}' & 0 \\ 0 & 0 & 0 & 0 & 0 & 0 & 0 & 0 & h_{n-1} & h_{n-1}' & -h_{n-1}' \\ 0 & 0 & 0 & 0 & 0 & 0 & 0 & 0 & f_{n-1} & -g_{n-1} & g_{n-1}' \end{vmatrix} = 0. \tag{6}$$

Substituting equations (3, 4) into the above determinant (6), the frequencies of IO and SO phonon could be solved. When ω was worked out, *via* equation (3), it was easy to

obtain the values of the dielectric functions $\varepsilon_i(\omega)$. Through equations (2), A_i and B_i ($i = 2,3$ to $n-1$) can be expressed by A_1 as

$$\begin{cases} A_i = \frac{M_{2i-3}}{M_0} A_1 \\ B_i = \frac{M_{2i-2}}{M_0} A_1 \end{cases}, \; i = 2,3 \text{ to } n-1 \tag{7}$$

$$B_n = \frac{M_{2n-3}}{M_0} A_1, \tag{8}$$

$$B_1 = A_n = 0 \tag{9}$$

with

$$M_0 = \begin{vmatrix} -h_1 & -h_1' & 0 & 0 & 0 & 0 & 0 & 0 & 0 & 0 \\ -f_1' & g_1' & 0 & 0 & 0 & 0 & 0 & 0 & 0 & 0 \\ h_2 & h_2' & -h_2 & -h_2' & 0 & 0 & 0 & 0 & 0 & 0 \\ f_2 & -g_2 & -f_2' & g_2' & 0 & 0 & 0 & 0 & 0 & 0 \\ 0 & 0 & 0 & 0 & \ldots & 0 & 0 & 0 & 0 & 0 \\ 0 & 0 & 0 & 0 & 0 & h_{n-2} & h_{n-2}' & -h_{n-2} & -h_{n-2}' & 0 \\ 0 & 0 & 0 & 0 & 0 & f_{n-2} & -g_{n-2} & -f_{n-2}' & g_{n-2}' & 0 \\ 0 & 0 & 0 & 0 & 0 & 0 & 0 & h_{n-1} & h_{n-1}' & -h_{n-1}' \end{vmatrix}, \tag{10}$$

$$M_j = \begin{vmatrix} -h_1 & -h_1' & 0 & 0 & -h_1 & 0 & 0 & 0 & 0 & 0 \\ -f_1' & g_1' & 0 & 0 & -f_1 & 0 & 0 & 0 & 0 & 0 \\ h_2 & h_2' & -h_2 & -h_2' & 0 & 0 & 0 & 0 & 0 & 0 \\ f_2 & -g_2 & -f_2' & g_2' & 0 & 0 & 0 & 0 & 0 & 0 \\ 0 & 0 & 0 & 0 & \ldots & 0 & 0 & 0 & 0 & 0 \\ 0 & 0 & 0 & 0 & 0 & h_{n-2} & h_{n-2}' & -h_{n-2} & -h_{n-2}' & 0 \\ 0 & 0 & 0 & 0 & 0 & f_{n-2} & -g_{n-2} & -f_{n-2}' & g_{n-2}' & 0 \\ 0 & 0 & 0 & 0 & 0 & 0 & 0 & h_{n-1} & h_{n-1}' & -h_{n-1}' \end{vmatrix} \tag{11}$$

where M_0 and M_j are $(2n-3)\times(2n-3)$ determinants. It should be noticed that column matrix $(-h_1, -f_1, 0, 0, ..., 0, 0, 0)$ was at the jth column in M_j. During the calculation procedure, the Cramer rule for solving the linear equations was employed. Using equations (7, 8, 9), the phonon potential function (1) can be given as

$$\phi(\mathbf{r}) = \begin{cases} A_1 M_0 r^l Y_{lm}(\theta,\varphi) & 0 < r \le r_1 \\ A_1(M_1 r^l + M_2 r^{-l-1}) Y_{lm}(\theta,\varphi) & r_1 < r \le r_2 \\ \ldots & \ldots \\ A_1(M_{2i-3} r^l + M_{2i-2} r^{-l-1}) Y_{lm}(\theta,\varphi) & r_{i-1} < r \le r_i \\ \ldots & \ldots \\ A_1 M_{2n-3} r^{-l-1} Y_{lm}(\theta,\varphi) & r_{n-1} < r < \infty \end{cases}. \tag{12}$$

The polarization fields for the IO and SO phonon modes of the system are

$$\mathbf{P}_{lm}^{\mathrm{IO,SO}} = \begin{cases} A_1 \frac{1-\varepsilon_1}{4\pi} \nabla[M_0 r^l Y_{lm}(\theta,\varphi)] & 0 < r \le r_1 \\ A_1 \frac{1-\varepsilon_2}{4\pi} \nabla[(M_1 r^l + M_2 r^{-l-1}) Y_{lm}(\theta,\varphi)] & r_1 < r \le r_2 \\ \ldots & \ldots \\ A_1 \frac{1-\varepsilon_i}{4\pi} \nabla[(M_{2i-3} r^l + M_{2i-2} r^{-l-1}) Y_{lm}(\theta,\varphi)] & r_{i-1} < r \le r_i \\ \ldots & \ldots \\ A_1 \frac{1-\varepsilon_d}{4\pi} \nabla[M_{2n-3} r^{-l-1} Y_{lm}(\theta,\varphi)] & r_{n-1} < r < \infty. \end{cases} \tag{13}$$

Using the Green's first identity

$$\int_V \nabla\phi \cdot \nabla\varphi \mathrm{d}^3\mathbf{r} = -\int_V \phi \nabla^2 \varphi \mathrm{d}^3\mathbf{r} + \int_S \phi \frac{\partial \varphi}{\partial n} \mathrm{d}a, \tag{14}$$

then we obtain the orthogonal relation for $\mathbf{P}_{lm}^{\mathrm{IO,SO}}$

$$\begin{aligned} &\int \mathbf{P}_{l'm'}^{IO,SO^*} \cdot \mathbf{P}_{lm}^{\mathrm{IO,SO}} \mathrm{d}^3\mathbf{r} = \\ &\sum_{i=1}^{n-1} \frac{(1-\varepsilon_i)^2}{16\pi^2} \int_{V_i} \nabla\phi_{il'm'} \cdot \nabla\phi_{ilm} \mathrm{d}^3\mathbf{r} \\ &= \frac{|A_1|^2}{16\pi^2} \sum_{i=1}^{n-1} (1-\varepsilon_i)^2 \int_{S_i} \phi_{il'm'} \frac{\partial \phi_{ilm}}{\partial \mathrm{n}} \mathrm{d}a \\ &= \frac{|A_1|^2}{16\pi^2} \sum_{i=1}^{n-1} (1-\varepsilon_i)^2 [l M_{2i-3}^2 (r_i^{2l-1} - r_{i-1}^{2l-1}) \\ &\quad - M_{2i-3} M_{2i-2} (r_i^{-2} - r_{i-1}^{-2}) \\ &\quad - (l+1) M_{2i-2}^2 (r_i^{-2l-3} - r_{i-1}^{-2l-3})] \\ &\quad + (1-\varepsilon_1)^2 l M_0^2 r_1^{2l-1}\} \delta_{l'l} \delta_{m'm}. \end{aligned} \tag{15}$$

In order to derive the free-phonon Hamiltonian, we need the dynamic equation of motion of the crystal lattice [17]:

$$\mu \ddot{\mathbf{u}} = \mu\omega_0^2 \mathbf{u} + e\mathbf{E}_{loc}, \tag{16}$$

$$\mathbf{P} = n^* e \mathbf{u} + n^* \alpha \mathbf{E}_{loc}, \tag{17}$$

where μ is the reduced mass of the ion pair and $\mathbf{u} = \mathbf{u}_+ - \mathbf{u}_-$ is the relative displacement of the positive and negative ions, ω_0 is the frequency associated with the short-range force between ions, n^* is the number of ion pairs per unit volume, and α is the electronic polarizability per ion pair, $\mathbf{E}_{loc}$ is the local field at the position of the ions.

The Hamiltonian of the free vibration is given by

$$H_{\mathrm{ph}} = \frac{1}{2} \int [n^* \mu \, \dot{\mathbf{u}} \cdot \dot{\mathbf{u}} + n^* \mu \omega_0^2 \mathbf{u} \cdot \mathbf{u} - n^* e \mathbf{u} \cdot \mathbf{E}_{loc}] \mathrm{d}^3\mathbf{r}, \tag{18}$$

via equations (16, 17), we have [8,9]

$$\mathbf{E}_{loc} = \frac{\mu}{e} (\omega_0^2 - \omega^2) \mathbf{u}, \tag{19}$$

$$\mathbf{u} = \frac{\mathbf{P}}{n^* e [1 + (\alpha\mu/e^2)(\omega_0^2 - \omega^2)]}. \tag{20}$$

Substituting equations (19, 20) into equation (18), we then get the Hamiltonian for the IO phonon or the SO phonon

$$\begin{aligned} H_{\mathrm{IO,\,SO}} = \frac{1}{2} \int \Bigg[& n^* \mu \left(\frac{1}{n^* e [1 + (\alpha\mu/e^2)(\omega_0^2 - \omega^2)]} \right)^2 \dot{\mathbf{P}}^* \cdot \dot{\mathbf{P}} \\ & + n^* \mu \omega^2 \left(\frac{1}{n^* e [1 + (\alpha\mu/e^2)(\omega_0^2 - \omega^2)]} \right)^2 \mathbf{P}^* \cdot \mathbf{P} \Bigg] \mathrm{d}^3\mathbf{r}. \end{aligned} \tag{21}$$

Using the orthogonal relation of the polarization vector (15) and choosing

$$|A_1|^{-2} = \frac{1}{4\pi\omega^2}\Bigg\{\left(\frac{1}{\varepsilon_1-\varepsilon_{10}}-\frac{1}{\varepsilon_1-\varepsilon_{1\infty}}\right)^{-1} lM_0^2 r_1^{2l-1} + \sum_{i=2}^{n-1}\Bigg[\left(\frac{1}{\varepsilon_i-\varepsilon_{i0}}-\frac{1}{\varepsilon_i-\varepsilon_{i\infty}}\right)^{-1} \times \left[lM_{2i-3}^2(r_i^{2l-1}-r_{i-1}^{2l-1}) - M_{2i-3}M_{2i-2} \times (r_i^{-2}-r_{i-1}^{-2}) - (l+1)M_{2i-2}^2(r_i^{-2l-3}-r_{i-1}^{-2l-3})\right]\Bigg]\Bigg\} \tag{22}$$

can make $\mathbf{P}_{lm}^{\mathrm{IO,SO}}$ form orthonormal and complete sets, which can be used to express the IO and SO phonon field $H_{\mathrm{IO,SO}}$ and the electron-phonon interaction Hamiltonian $H_{e-\mathrm{IO,SO}}$. The IO and SO phonon field was given as

$$H_{\mathrm{IO,SO}} = \sum_{lm}\hbar\omega\left[c_{lm}^{\dagger}c_{lm}+\frac{1}{2}\right], \tag{23}$$

where $c_{lm}^{\dagger}$ and c_{lm} were creation and annihilation operator for IO and SO phonon of the (l,m)th mode. They satisfied the commutative rules for bosons

$$\begin{aligned}&[c_{lm},\, c_{l'm'}^{\dagger}] = \delta_{l'l}\delta_{m'm},\\ &[c_{lm},\, c_{l'm'}] = [c_{lm}^{\dagger},\, c_{l'm'}^{\dagger}] = 0.\end{aligned} \tag{24}$$

The Fröhlich Hamiltonian describing the interaction between the electron and the IO and SO phonon was given by

$$H_{e-\mathrm{IO,SO}} = -\sum_{lm} I_l^{\mathrm{IO,SO}}(r)Y_{lm}(\theta,\varphi)\left[c_{lm}+c_{lm}^{\dagger}\right], \tag{25}$$

where $I_l^{\mathrm{IO,SO}}(r)$ was the coupling function which was defined as

$$I_l^{\mathrm{IO,SO}}(r) = f_l \times \begin{cases} M_0 r^l & r \le r_1 \\ (M_1 r^l + M_2 r^{-l-1}) & r_1 < r \le r_2 \\ \cdots & \cdots \\ (M_{2i-3}r^l + M_{2i-2}r^{-l-1}) & r_{i-1} < r \le r_i \\ \cdots & \cdots \\ M_{2n-3}r^{-l-1} & r_{n-1} < r < \infty \end{cases} \tag{26}$$

with

$$|f_l|^2 = 4\pi\hbar\omega e^2\Bigg\{\left(\frac{1}{\varepsilon_1-\varepsilon_{10}}-\frac{1}{\varepsilon_1-\varepsilon_{1\infty}}\right)^{-1} lM_0^2 r_1^{2l-1} + \sum_{n-1}^{i=2}\Bigg[\left(\frac{1}{\varepsilon_i-\varepsilon_{i0}}-\frac{1}{\varepsilon_i-\varepsilon_{i\infty}}\right)^{-1} \times \left[lM_{2i-3}^2\left(r_i^{2l-1}-r_{i-1}^{2l-1}\right) - M_{2i-3}M_{2i-2}\left(r_i^{-2}-r_{i-1}^{-2}\right) - (l+1)M_{2i-2}^2\left(r_i^{-2l-3}-r_{i-1}^{-2l-3}\right)\right]\Bigg]\Bigg\}^{-1}. \tag{27}$$

3 Numerical results and discussion

In order to see more clearly the behaviors of the IO and SO phonon modes and their interaction with the electron, numerical calculations on three layers spherical system of CdS/HgS/H_2O and four layers spherical system of CdS/HgS/CdS/H_2O have been performed. The material parameters of the system are [13]: $\varepsilon_{0,\mathrm{CdS}} = 9.1$, $\varepsilon_{\infty,\mathrm{CdS}} = 5.5$, $\omega_{LO,\mathrm{CdS}} = 57.2$ meV, $\varepsilon_{0,\mathrm{HgS}} = 18.2$, $\varepsilon_{\infty,\mathrm{HgS}} = 11.36$, $\omega_{LO,\mathrm{HgS}} = 27.8$ meV, $\varepsilon_{d,\mathrm{H_2O}} = 1.78$.

Figures 2 and 3 show the dispersion of the IO and SO modes in the CdS/HgS/H_2O system and the CdS/HgS/CdS/H_2O system, respectively. Other than the multilayer planar QW system [4–6], in which the IO and SO phonon frequency was the continuum function of wave-vector, the IO and SO frequencies in multilayer spherical nanostructures were discrete functions of the quantum number l. In Figure 2, we can see that the dispersion of mode 3 was more significant compared with the other two modes. Furthermore, it can be seen that only three frequency solutions for the CdS/HgS/H_2O system exist, the highest frequency mode 3 is between $\omega_{TO,\mathrm{CdS}}$ and $\omega_{LO,\mathrm{CdS}}$, and the frequencies of the other two modes 1, 2 are between $\omega_{TO,\mathrm{HgS}}$ and $\omega_{LO,\mathrm{HgS}}$. From Figure 3, it is observed that there exist five solutions for the CdS/HgS/CdS/H_2O system, three frequencies of them are between $\omega_{TO,\mathrm{HgS}}$ and $\omega_{LO,\mathrm{HgS}}$, the frequencies of the other two are between $\omega_{TO,\mathrm{CdS}}$ and $\omega_{LO,\mathrm{CdS}}$. It is interesting to note that the frequencies of the modes 1 and 2 approach the same value while the frequencies of the modes 3 and 4 approach another value with the increase of l. This can be explained as following: with the increase of l, the phonon potential functions becomes steeper, which make the potential coupling between every interface less and less likely, so the dispersion frequencies approach the frequencies value of single CdS/HgS heterostructures. The mode 5 was the SO mode, which can be seen clearly in Figure 7.

The electron-IO (SO) phonon coupling functions $I_l(r)$ of these two systems as the function of r for $l = 1$ were plotted in Figure 4 and 5, respectively. From them, it was clearly seen where every mode was localized. In Figure 4, we can observe that the modes 1 and 3 mainly localized at the interface $r = 2.35$ nm, and mode 2 was bound at the surface, which can be looked at as a SO phonon. The SO phonon contribution to $I_l(r)$ was between that of modes 1, 2 for $l = 1$ and exceeded that of the other two modes when $l > 1$ which was quite obvious in Figure 6. Through Figure 5, it can be found that modes 2 and 3 were mainly localized at the first interface, $r = 2.35$ nm, and mode 1 was mainly bound at the second interface $r = 3.35$ nm. For modes 4, 5, because the potential coupling is strong for the quantum number $l = 1$, the potential distribution at the three interface were average comparatively, but in Figure 7 it can be seen that the mode 4 was mainly bound at the second interface, and the mode 5 was the SO phonon mode which was mainly localized at the surface when $l > 3$.

In Figure 6 and Figure 7, we show the absolute values $|I_l(r)|$ as a function of the quantum number l for the

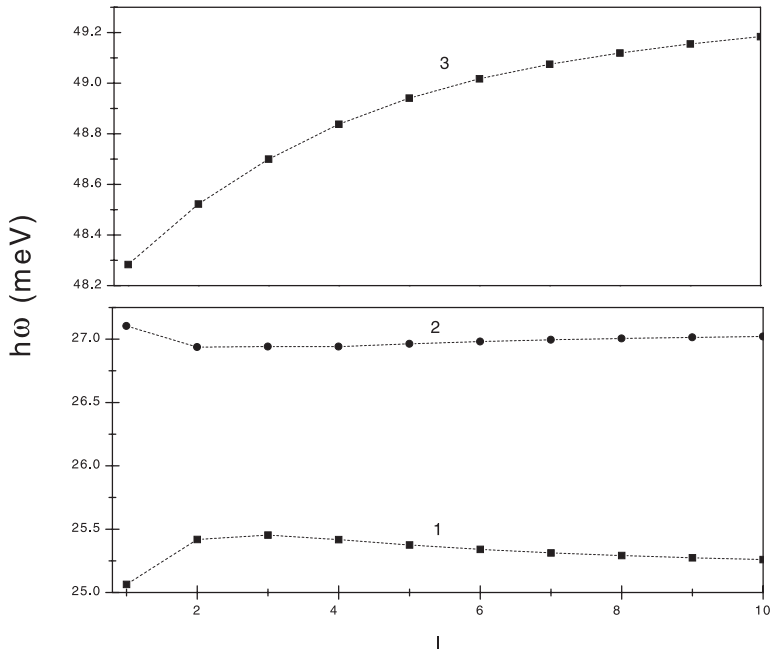

Fig. 2. Dispersion curves of the IO and SO phonon modes for the spherical CdS/HgS/H_2O system with thicknesses 2.35 nm/4.35 nm/∞.

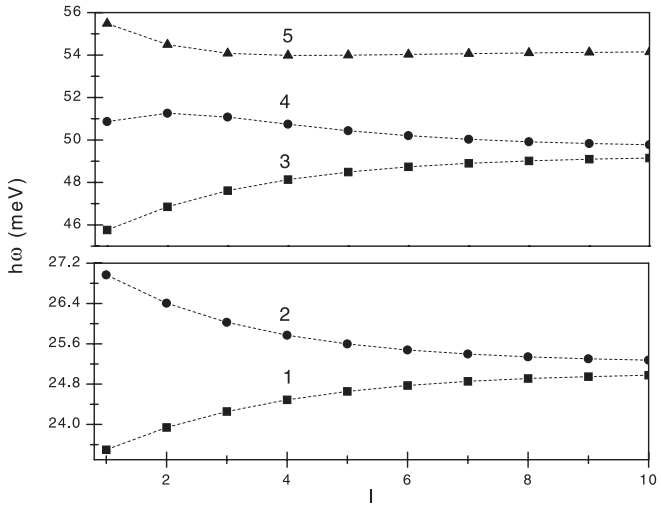

Fig. 3. Dispersion curves of the IO and SO phonon modes for the spherical CdS/HgS/CdS/H_2O system with thicknesses 2.35 nm/3.35 nm/5.35 nm/∞.

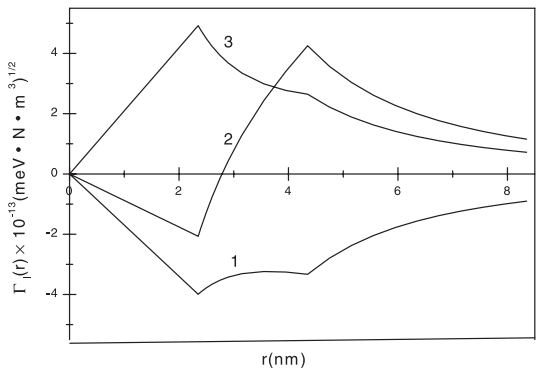

Fig. 4. The coupling function $\Gamma_l(r)$ as a function of r for the spherical CdS/HgS/H_2O system with thicknesses 2.35 nm/4.35 nm/∞, and $l = 1$.

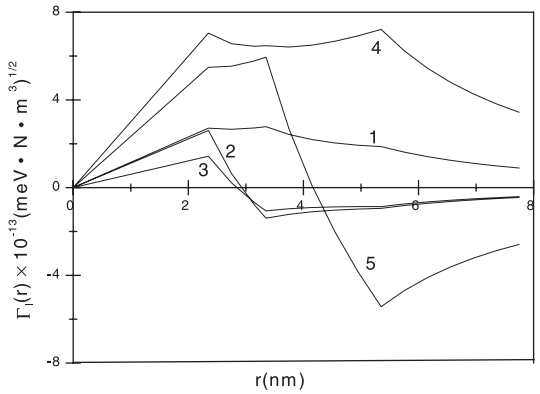

Fig. 5. The coupling function $\Gamma_l(r)$ as a function of r for the spherical CdS/HgS/CdS/H_2O system with thicknesses 2.35 nm/3.35 nm/5.35 nm/∞, and $l = 1$.

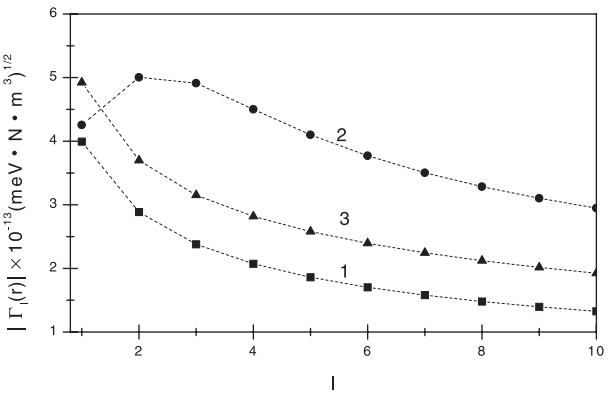

Fig. 6. Absolute values $|\Gamma_l(r)|$ as functions of the quantum number l for the CdS/HgS/H_2O system with the same structure as in Figure 2.

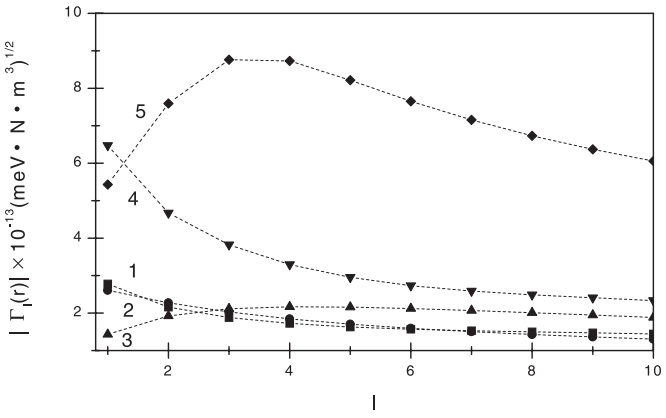

Fig. 7. Absolute values $|\Gamma_l(r)|$ as functions of the quantum number l for the CdS/HgS/CdS/H_2O system with the same structure as in Figure 3.

CdS/HgS/H_2O system and the CdS/HgS/CdS/H_2O system, respectively. According to Figure 3, we have chosen $r = 2.35$ nm for modes 1, 3 and $r = 4.35$ nm for mode 2 in Figure 6. The figure shows that the values of modes 1 and 3 decrease monotonously with the increase of l, while that of mode 2 has a maximum value at $l = 2$. It was also noticed that the coupling between the electron-SO phonon were more drastic than that of the other two except for $l = 1$. According to Figure 4, we have chosen $r = 2.35$ nm for modes 2, 3, $r = 3.35$ nm for modes 1, 4, and $r = 5.35$ nm for mode 5 in Figure 7. $|\Gamma_l(r)|$ of modes 1, 2, 4 decrease, and that of mode 3 has a slight increase as the increase of l monotonously, while that of mode 5 increases to a maximum value at $l = 2$, then decreases after it. In the whole range of l, except for $l = 1$, the electron-SO phonon coupling is more significant.

4 Summary and conclusions

In this paper, the IO and SO phonon modes, electron-IO (SO) phonon Fröhlich interaction Hamiltonian in an n-layer shell spherical system have been investigated in detail. Numerical calculation on three and four layer spherical systems have been performed. The main results were:

1. For CdS/HgS/H_2O systems, there were three frequency solutions for the IO (SO) phonon modes, two of them were IO modes, and one was the SO mode. The electron-IO (SO) phonon interaction for a smaller quantum number l were more important, and the SO phonon has a significant contribution, compared with the IO phonon, to $\Gamma_l(r)$.

2. For four layer CdS/HgS/CdS/H_2O systems, there were five frequency solutions for IO (SO) phonon modes, two frequency values of them were between $\omega_{TO,\mathrm{CdS}}$, and $\omega_{LO,\mathrm{CdS}}$, three frequency values lie between $\omega_{TO,\mathrm{HgS}}$, and $\omega_{LO,\mathrm{HgS}}$. Furthermore, it has been found that, with the increase of l, the frequencies of two modes converge to the same value, whilst that of another two modes converge to a different value. A reason for this observation has also been given. We also found that there were two IO modes on each interface and only one SO mode on the surface, and small l and SO mode make important contributions to the electron-IO (SO) interaction.

From the results of three and four layer spherical systems, it is reasonable to draw a conclusion, for n-layers CdS/HgS/.../H_2O spherical system, that the number of IO (SO) modes was $2n - 3$ ($n \geq 3$). There is only one SO mode and $2n-4$ IO phonon modes whose frequencies approach the frequencies of single heterostructure as l approach infinity in the system. On each interface there exits two IO phonon modes, the frequency of one is between $\omega_{TO,\mathrm{CdS}}$, and $\omega_{LO,\mathrm{CdS}}$, the frequency of the other one is between $\omega_{TO,\mathrm{HgS}}$, and $\omega_{LO,\mathrm{HgS}}$.

This work is supported by Guangdong Provincial Natural Science Foundation of China.

References

1. A. Mews, A. Eychmüller, M. Giersig, D. Schooss, H. Weller, J. Phys. Chem. **98**, 934 (1994)
2. A. Eychmüller, A. Mews, H. weller, Chem. Phys. Lett. **208**, 59 (1993)
3. A. Eychmüller, T. Vossmeyer, A. Mews, H. Weller, J. Lumin. **58**, 223 (1994)
4. N. Mori, T. Ando, Phys. Rev. B **40**, 6175 (1989)
5. Shi Jun-jie, Pan Shao-hua, Phys. Rev. B **51**, 17 681 (1995)
6. Shi Jun-jie, Pan Shao-hua, J. Appl. Phys. **80**, 3863 (1996)
7. N.C. Constantinou, B.K. Ridley, Phys. Rev. B **41**, 10 627 (1990)
8. Hong-Jing Xie, Chuan-Yu Chen, Ben-Kun Ma, J. Phys. Cond. Matt. **12**, 8263 (2000)
9. Hong-Jing Xie, Chuan-Yu Chen, Ben-Kun Ma, Phys. Rev. B **61**, 4827 (2000)
10. S.N. Klimin, E.P. Pokatilov, V.M. Fomin, Phys. Stat. Sol. (b) **184**, 373 (1994)
11. M.C. Klein, F. Hache, D. Ricard, C. Flytzanix, Phys. Rev. B **42**, 11 123 (1990)
12. E. Roca, C. Trallero-Giner, M. Cardona, Phys. Rev. B **49**, 13 704 (1994)
13. M. Tkach, V. Holovatsky, O. Voitsekhivska, M. Mikhalyova, Phys. Stat. Sol. (b) **203**, 373 (1997)
14. Kun Hung, Bangfen Zhu, Phys. Rev. B **38**, 13 377 (1988)
15. H. Rücker, E. Molinari, P. Lugli, Phys. Rev. B **44**, 3463 (1991)
16. H. Rücker, E. Molinari, P. Lugli, Phys. Rev. B **45**, 6747 (1992)
17. M. Born, K. Huang, *Dynamical Theory of Crystal Lattice* (Clarenden Press, Oxford, 1954)